AIAA-2001-1431

COUPLED AERODYNAMIC AND STRUCTUAL SENSITIVITY ANALYSIS OF A HIGH-SPEED CIVIL TRANSPORT

B. H. Mason*
Analytical and Computational Methods Branch

and

J. L. Walsh†
Multidisciplinary Optimization Branch
NASA Langley Research Center
Hampton, VA 23681-2199

Abstract

An objective of the High Performance Computing and Communication Program at the NASA Langley Research Center is to demonstrate multidisciplinary shape and sizing optimization of a complete aerospace vehicle configuration by using high-fidelity, finite-element structural analysis and computational fluid dynamics aerodynamic analysis. In a previous study, a multi-disciplinary analysis system for a high-speed civil transport was formulated to integrate a set of existing discipline analysis codes, some of them computationally intensive. This paper is an extension of the previous study, in which the sensitivity analysis for the coupled aerodynamic and structural analysis problem is formulated and implemented. Uncoupled stress sensitivities computed with a constant load vector in a commercial finite element analysis code are compared to coupled aeroelastic sensitivities computed by finite differences. The computational expense of these sensitivity calculation methods is discussed.

Nomenclature

a_C	Aerodynamic cruise load vector
a_M	Aerodynamic maneuver (converged) load vector
f_A	Augmented structural load vector
f_C	Structural cruise load vector
f_M	Structural maneuver (converged) load vector
s_0	Unloaded shape vector
s_C	Cruise shape vector
s_M	Maneuver (converged) shape vector
σ_A	Stress vector (due to augmented loads)
u_0	Displacement (unloaded to cruise shape) vector
u_A	Augmented displacement vector
u_C	Cruise displacement vector
u_M	Maneuver (converged) displacement vector
v	Independent design variables
w_C	Cruise weight
w_M	Maneuver weight
K_C	Stiffness matrix (cruise shape)
K_0	Stiffness matrix (unloaded shape)
LF	Inertial load factor (g's)

Introduction

One of the objectives of the High Performance Computing and Communication Program (HPCCP) at NASA Langley Research Center (LaRC) has been to promote the use of advanced computing techniques to rapidly solve the problem of multidisciplinary optimization of aerospace vehicles. In 1992, the HPCCP Computational Aerosciences (CAS) team at LaRC began a multidisciplinary analysis and optimization software project. Initially, the focus of the CAS project was on the software integration system used to integrate fast analysis on a simplified design application. The sample application for this project was a High Speed Civil Transport (HSCT). Over the years, progressively more complex engineering analyses have been incorporated. In 1997, the sample application shifted to a more realistic model and higher fidelity analyses and is referred to as the HSCT4.0 application. The analysis formulation and preliminary results from the HSCT4.0 application were presented in Refs. 1 and 2, respectively. However, sensitivity analysis was not performed in Refs. 1 and 2.

As discussed in Refs. 1 and 2, analytical sensitivities can be obtained from most of the analysis codes by using automatic differentiation tools. However, Ref. 1 discussed the one major stumbling block in formulating the sensitivity analysis—obtaining sensitivity derivatives of the converged aeroelastic loads and using those derivatives in a commercial finite element code. The aerodynamic pressures and

* Aerospace Engineer, Member AIAA
† Senior Research Engineer, Senior Member AIAA

structural deformations in the wing shape are mutually dependent. Because of this coupling between aerodynamic and structural responses, the sensitivity of the aeroelastic loads is difficult to compute. Researchers use one of two methods to compute these aeroelastic sensitivity derivatives. For the first method, researchers assume that the aeroelastic loads are constant and then use exiting methods to obtain sensitivity derivatives. In the second method, researchers assume the loads vary and use finite differences to obtain sensitivity derivatives. There has been some research[3-5] using the global sensitivity equations (GSE[6]) to account for the coupling of aerodynamics and structures. In Refs. 4 and 5, the GSE were applied to simplified HSCT models to compute derivatives of aerodynamic coefficients. In this paper, the effects of the coupled aeroelastic loads on the computation of stress sensitivities will be examined.

In Refs. 1 and 2, the HSCT4.0 analysis consisted of an integrated set of discipline codes and interface codes. These codes were implemented in a CORBA-Java computing environment known as CJOPT[7]. The present research does not use the CJOPT system; instead, the discipline codes and interface codes are implemented in the Phoenix Integration, Inc.'s ModelCenter®[8]. Implementation of the codes in ModelCenter® is not discussed in this paper. The work presented in the current paper is referred to as the HSCT4.1 application.

In the HSCT4.1 application, the coupling of the aeroelastic loads in the stress derivatives is important because both shape and structural design variables are used in the sensitivity analysis. The present paper will quantify the effect of aeroelastic coupling on stresses. Coupled stress sensitivities obtained by finite difference techniques (with loads varying) are compared with un-coupled stress sensitivities obtained from a commercial finite element code (with loads held constant).

First, an overview of the model and analysis will be presented. Next, the coupled and uncoupled stress sensitivity analysis formulation will be presented. Finally, sample results for both the coupled and uncoupled stress sensitivities are compared for both shape and structural design variables.

Overview

HSCT 4.1 Model

The HSCT4.1 application uses the same linear aerodynamic and finite element models as the HSCT4.0 application described in Refs. 1 and 2. The linear aerodynamics grid and the finite element model used for HSCT4.1 are shown in Figs. 1 and 2, respectively. An aerodynamic surface grid of approximately 1100 grid points is used in the linear aerodynamics code (USSAERO)[9]. The aerodynamic model does not include engines. The GENESIS®[10] finite element analysis code (a product of VR&D, Inc.) uses the 40,000 degree-of-freedom (DOF) FEM for displacement and stress response calculations. In this FEM, the engines are modeled as masses on beam elements. Seven laterally symmetric load conditions are used— one cruise load condition and six maneuver conditions (three at +2.5g and three at -1.0g). Note that the taxi condition used in Refs. 1 and 2 is not used in the present work.

Fig. 1. HSCT4.1 linear aerodynamic model.

Fig. 2. HSCT4.1 finite element model.

Optimization Problem Description

The objective function of the HSCT4.1 optimization problem is to minimize the aircraft gross takeoff weight (GTOW) subject to stress constraints. The HSCT4.1 application has 271 design variables for optimization—244 structural thickness variables and 27 shape variables. To limit the number of independent structural design variables, the optimization model is divided into 61 design variable zones. Each zone consists of several finite elements. Thirty-nine zones are located on the fuselage, and twenty-two zones are located on the wing (half are on the upper surface and the other half are on the lower surface). Within each zone, four structural design variables are used. These structural design variables consist of three ply-thickness variables (a 0^o fiber variable, a 45^o fiber variable, and a 90^o fiber variable with a dependent -45^o fiber variable set equal to the 45^o variable) and a core thickness variable. The 0^o and 90^o ply orientations at various locations on the model and the composite laminate stacking sequences are shown in Fig. 3.

The 27 shape design variables are divided into two sets. The first set contains 9 planform design variables– the root chord, the outboard break chord, the tip chord, the distance from the semispan to the outboard break, the leading edge sweep of the inboard wing panel, the leading edge sweep of the outboard wing panel, the total projected area of the wing, the fuselage nose length, and the fuselage tail length. The second set

consists of three sets of six variables that control the camber, thickness, and shear of the wing airfoil.

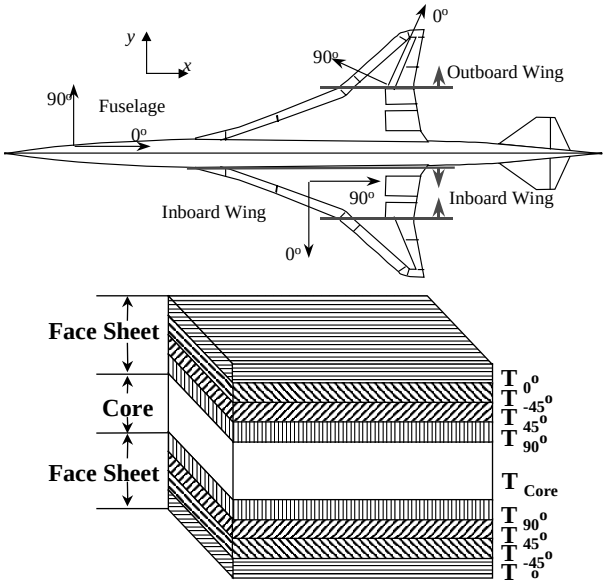

Fig. 3. Ply orientations and composite laminate stacking sequence.

HSCT4.1 *Analysis* Process

As discussed in Refs. 1 and 2, the HSCT4.0 analysis is formulated as a sequence of processes in the data flow diagrams, as shown in Fig. 4. The HSCT4.1 analysis is focused on the difficult aerodynamic-structures analysis-coupling problem and uses the analysis processes shown by shaded circles in Fig. 4. By convention, this paper uses italics for process names from Fig. 4.

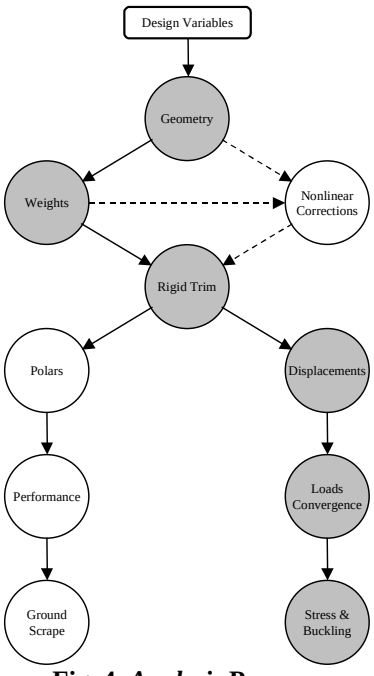

Fig. 4. *Analysis* Process.

The HSCT 4.1 *Analysis* process is started from the top of the data flow (Fig. 4) where the design variable values are prescribed. First, the *Geometry* process is used to derive updated geometric grids and FEM section properties from the design variables. Next, the *Weights* process uses the derived FEM grid and section properties to calculate detailed weights and the center of gravity (c.g.) locations for specified flight conditions. Theoretical FEM weights are computed for each node from the FEM data. A reference as-built weight increment is added to the theoretical FEM weight at each node to produce the as-built weight.

Next the *Rigid Trim* process is executed for the cruise condition to determine the configuration angle of attack and the tail deflection angle that combine to yield a lift equal to the weight, with no net pitching moment. The linear aerodynamics code is used to compute the trimmed aerodynamic pressures on the cruise shape aerodynamic grid. These pressures are then transferred from the aerodynamic grid points to the FEM nodal forces in the z-direction. Inertial forces (nodal weights times g-factor) are added to the aerodynamic forces to create the structural load vector. This structural load vector is used by the *Displacements* process to compute the unloaded shape of the aircraft (see Appendix A for further details). These cruise displacements are saved as a reference set for the *Loads Convergence* process.

In the *Loads Convergence* process, aeroelastic trim calculations are performed for the six noncruise load conditions, to produce the aeroelastically converged loads on the aircraft (see Appendix B for further details). Forces representing cabin pressure are added to these converged loads and are multiplied by a factor of safety (1.5). These augmented loads are used in the *Stress & Buckling* process to compute stress and buckling constraints for all elements contained in the 61 design zones on the fuselage and wing. Buckling constraints are not considered in this paper.

HSCT4.1 Sensitivity Analysis Formulation

In this section, sensitivities (first order derivatives with respect to the design variables) are formulated for the objective function (GTOW) and the stress constraints. First, the weight sensitivities are formulated analytically. Then the stress sensitivities for both the coupled and uncoupled methods are formulated.

Weight Sensitivity Formulation

In the HSCT4.1 system, structural weight sensitivities are computed analytically from the finite element dimensions and material properties using chain rule differentiation. Non-structural weights (fuel, payload, and non-modeled structures) are assumed to be constant (*i.e.* non-structural sensitivities are zero).

Only shell elements are sized by the structural design variables. Because the weight of each of these

elements is a linear function of the structural design variables, the weight sensitivity for those elements with respect to a structural design variable is simply the element area multiplied by the number of plies and the density of that ply.

Element weight sensitivities with respect to the shape design variables are computed by chain rule differentiation of the equations defining the dimensions of the element (length for beams, area for shells, and volume for solid elements). The *Geometry* process is used to compute the derivatives of the node locations with respect to the shape design variables. Element weights and weight sensitivities are extrapolated to the finite element nodes by the weight code. The element weight sensitivities are totaled to obtain the GTOW sensitivity.

Stress Sensitivity Formulation

Structural stresses, σ_A, are functions of the displacements. Therefore, the stresses and stress sensitivity derivatives ($d\sigma_A/dv$) are defined as follows:

$$\sigma_A = \sigma_A(u_A) \tag{1}$$

$$\frac{d\sigma_A}{dv} = \frac{\partial\sigma_A}{\partial u_A}\frac{du_A}{dv} \tag{2}$$

The relationship between the stresses and the displacements are defined in GENESIS®; therefore, it is only necessary to study the displacement derivatives (du_A/dv). Linear static structural displacements at converged maneuver conditions (u_A) are computed within GENESIS® from the stiffness matrix (K_C) and the augmented loads (f_A) using Equations 3 and 4.

$$K_C\, u_A = f_A \tag{3}$$

$$u_A = [K_C]^{-1} f_A \tag{4}$$

Derivatives of u_A with respect to the design variable vector (v) are obtained by differentiating Equation 3:

$$K_C\frac{du_A}{dv} + \frac{dK_C}{dv}u_A = \frac{df_A}{dv} \tag{5}$$

Rearranging Equation 5 gives:

$$\frac{du_A}{dv} = [K_C]^{-1}\frac{df_A}{dv} - [K_C]^{-1}\frac{dK_C}{dv}u_A \tag{6}$$

In Equation 6, the displacement derivative is composed of two terms. One term requires the force derivative, which is derived from the coupled aerodynamic and structural analyses, and is referred to as the coupled sensitivity term in Equation 7.

$$\left.\frac{du_A}{dv}\right)_{Coupled} = [K_C]^{-1}\left\{\frac{df_A}{dv}\right\} \tag{7}$$

The other term requires the stiffness matrix derivative, which is determined from structural terms only, and is referred to as the uncoupled sensitivity term, Equation 8.

$$\left.\frac{du_A}{dv}\right)_{Uncoupled} = -[K_C]^{-1}\frac{dK_C}{dv}u_A \tag{8}$$

The relationship between structural design variables and the stiffness matrix can be set up as direct input to GENESIS®. The *Geometry* process was used to generate relationships between the nodes of the stiffness matrix and the shape design variables as another set of GENESIS® input. Therefore, the uncoupled sensitivity term (Equation 8) can be computed directly using the sensitivity analysis capability in GENESIS®.

The coupled sensitivity term (Equation 7) is similar to the displacement calculation equation (Equation 4). Therefore, GENESIS® can be used to compute the coupled sensitivity term in the displacement sensitivity equation from a linear static finite element displacement analysis using the load sensitivities as a nodal force vector. One complication of this method is that the sensitivities with respect to each design variable must be defined as a separate load case (*i.e.* one load case is required per design variable). Another complication is the fact that the augmented load sensitivity (df_A/dv) must be computed outside of GENESIS®.

The augmented loads (f_A) are computed from the converged maneuver loads (f_M), the factor of safety (1.5) and the cabin pressures (constant); therefore the derivatives of the augmented loads are:

$$\frac{df_A}{dv} = 1.5\frac{df_M}{dv}. \tag{9}$$

In the *Loads Convergence* process, the maneuver loads (f_M) and maneuver displacements (u_M) are mutually dependent. The nature of this dependency is discussed in Appendix B, and is represented in Equations 10 and 11:

$$u_M = u_M(f_M, v) \tag{10}$$

$$f_M = f_M(u_M, v) \tag{11}$$

Because of the coupling of f_M and u_M, computation of df_M/dv is complicated and beyond the scope of this paper. The total stress sensitivity derivative ($d\sigma_A/dv$) is obtained by substituting du_A/dv from Equation 6 into Equation 2. For the uncoupled stress sensitivity derivative, du_A/dv from Equation 8 are used in Equation 2 instead. In the next section, results are presented for analytically computed uncoupled stress sensitivities. Coupling effects are shown by parametric stress analyses in the next section.

HSCT4.1 Weight and Stress Results

Analysis results were presented in Ref. 2. To validate the HSCT4.1 *Analysis* process, loads convergence displacements and stress results from Ref. 2 for the baseline configuration were compared with HSCT4.1 results. The results from the two analyses agreed with each other. In Ref. 2, ten iterations were

used in the *Loads Convergence* process. Therefore, all results in this paper used ten iterations in the *Loads Convergence* process. Both parametrically- and analytically-computed GTOW and stress results are presented in this section.

Parametric studies were performed by perturbing one design variable at a time from its baseline value and then running the complete HSCT 4.1 *Analysis*. In the parametric studies, design variables are perturbed by a maximum of 1% from their baseline values.

Structural responses (r, referred to as analytical responses) are computed from Equation 12. Sensitivity analyses are used to compute first order derivatives of the response functions (dr/dv) at the baseline design point ($v_{Baseline}$).

$$r(v) = \frac{dr}{dv}\left(v - v_{Baseline}\right) + r_{Baseline} \qquad (12)$$

Due to the large number of design variables available for study, results for a small subset of the design variables are presented in this paper; four of the twenty-seven shape design variables (two chord lengths, one span length, and the wing planform area) are selected for study. Further, only two of the 244 structural design variables (ply thicknesses in the design variable zone at the wing break where the largest stresses occurred) are selected for study.

Weight Variations with Design Variables

Weight results are presented as the GTOW normalized by the baseline GTOW. GTOW is plotted as a function of the six selected design variables in Figs. 5 to 10. The analytic GTOW curves are computed using Equation 12 (linear approximations). Note that the weight sensitivity calculations do not involve aeroelastic coupling. The analytic curves agreed with the parametric curves. The GTOW axis is different in Figs. 5 to 8 (variations in shape variables) due to the large difference in the GTOW variations for each variable. As described in the Weight Sensitivity section and shown in Figs. 9 and 10 (variations in structural variables), weight is a linear function of the each of the structural design variables.

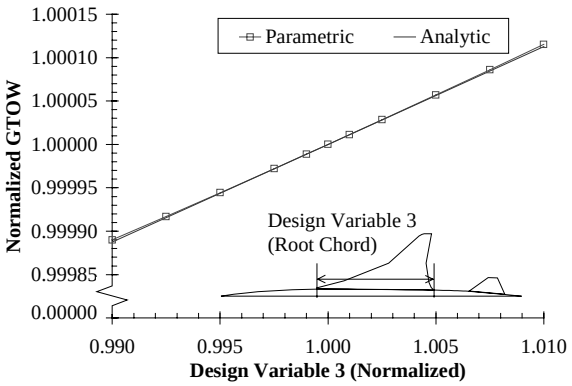

Fig. 5. GTOW variation with design variable 3.

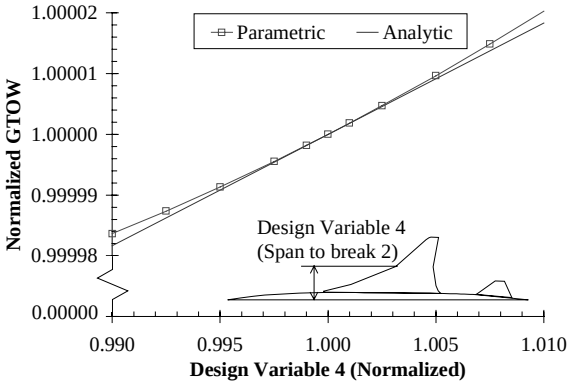

Fig. 6. GTOW variation with design variable 4.

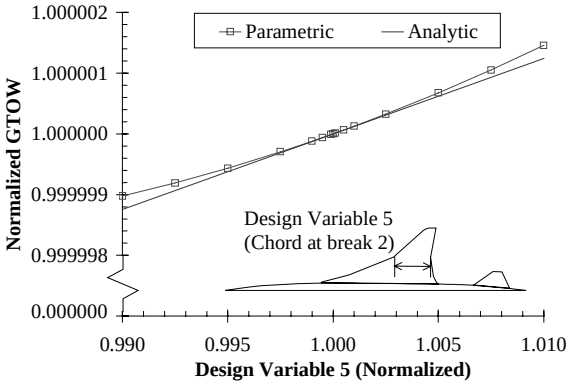

Fig. 7. GTOW variation with design variable 5.

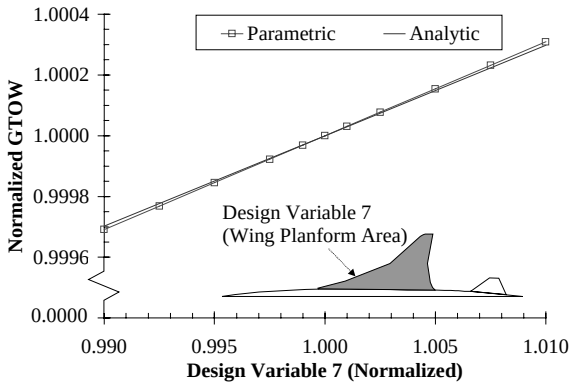

Fig. 8. GTOW variation with design variable 7.

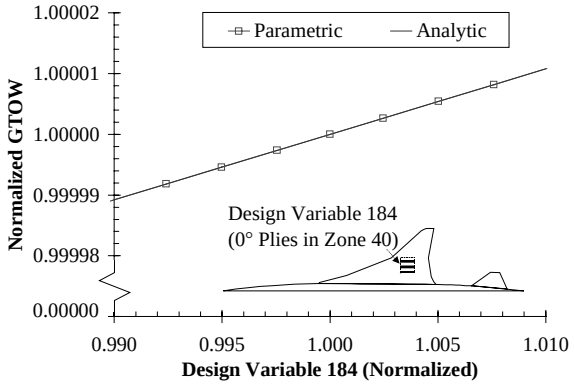

Fig. 9. GTOW variation with design variable 184.

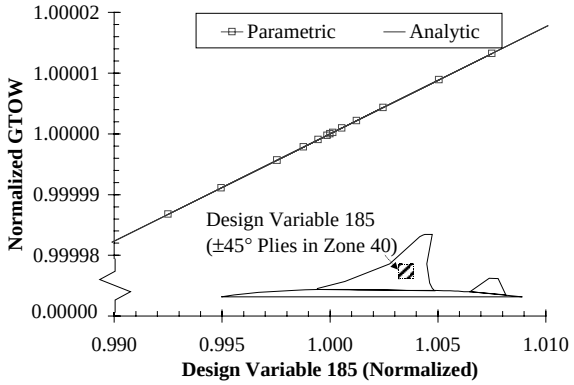

Fig. 10. GTOW variation with design variable 185.

Stress Variations with Design Variables

Stress results are presented as stress failure index (SFI) values (Ref. 2). In the *Analysis* process, stresses are computed for eight plies of 2260 sized elements for six load conditions. Due to the large number of results (108,480 responses), only subsets of these results are presented in this paper. Stress results are shown only for one of the three +2.5g maneuver load conditions and for three elements (see Fig. 11) with large stress responses.

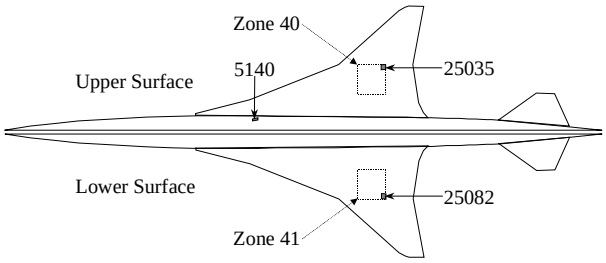

Fig. 11. Elements selected for stress responses.

In Figs. 12 to 29, parametrically and analytically computed SFI values are plotted as functions of the design variables. All analytical SFI curves are determined using Equation 12 where the uncoupled stress sensitivity (obtained from GENESIS® using Equations 2 and 8) is used for the response sensitivity term (dr/dv). In the following plots this stress sensitivity is represented as the slope of the analytic stress curve.

SFI responses for element 5140 (on the fuselage) are plotted in Figs. 12 to 17. The ranges of the SFI axes in Figs. 12 to 15 are identical for comparison purposes. The parametric SFI response curves in Figs. 12 to 15 are shallow curves (not quite linear). It is noted that the slope of the parametric curves at the baseline design point (normalized design variable value of 1.0) are different from the slope of the analytic (uncoupled) curve. The difference in the slopes varies from one variable to another, but in general the difference is significant. The ranges of the SFI axes in Figs. 16 and 17 are magnified from Figs. 12 to 15 because the sensitivity of the SFI in the fuselage is much smaller with respect to changes in the upper wing surface (zone 40) ply thicknesses. Because the sensitivity with respect to variables 184 and 185 is very small, the SFI response is more erratic. Some of this noise is the result of round-off error due to passing results from one analysis code to another using low-precision text output. This noise could also be due to the nonlinearity of the SFI response.

Note that the differences in the slopes of the parametric and analytic (uncoupled) SFI response curves are larger in Figs. 12 to 15 than in Figs. 16 and 17. Thus, the coupling effect (due to aeroelastic forces) seems to be larger for the shape design variables than for the structural design variables. The aeroelastic forces are a function of the weight and the HSCT shape. Shape variables affect both the shape and the weight, while the structural design variables only affect the weight. Therefore, the shape variables have a larger coupling effect for the SFI responses than the structural variables; a conclusion, which is supported by Figs. 12 to 17.

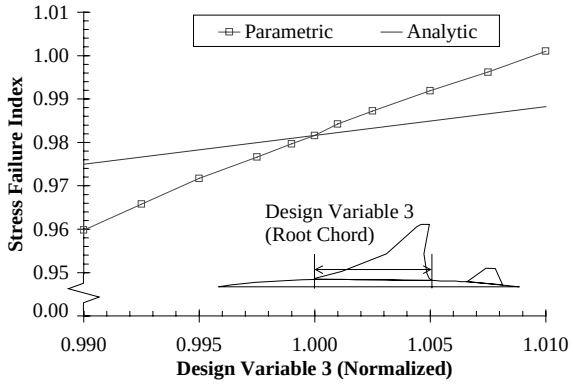

Fig. 12. SFI variation with design variable 3 for element 5140.

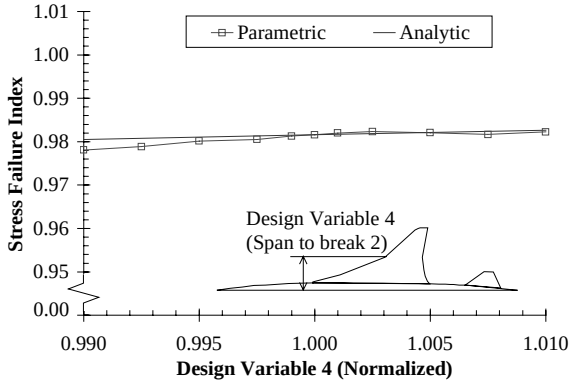

Fig. 13. SFI variation with design variable 4 for element 5140.

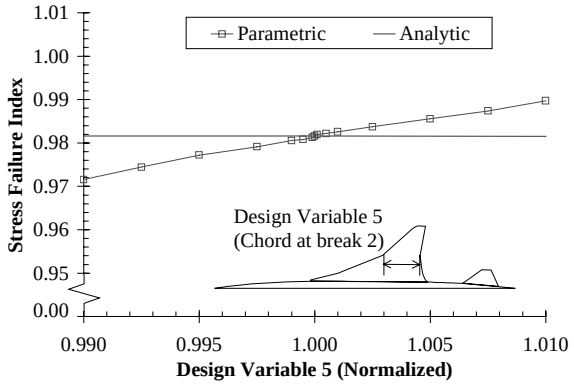

Fig. 14. SFI variation with design variable 5 for element 5140.

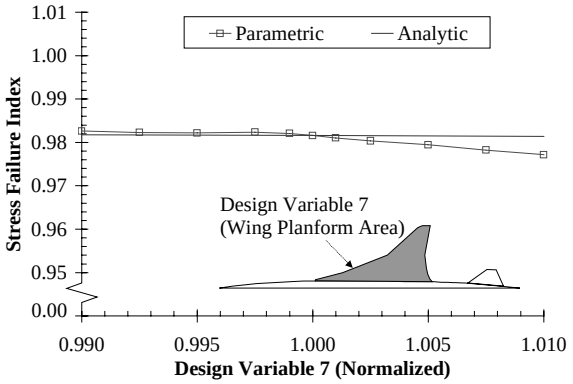

Fig. 15. SFI variation with design variable 7 for element 5140.

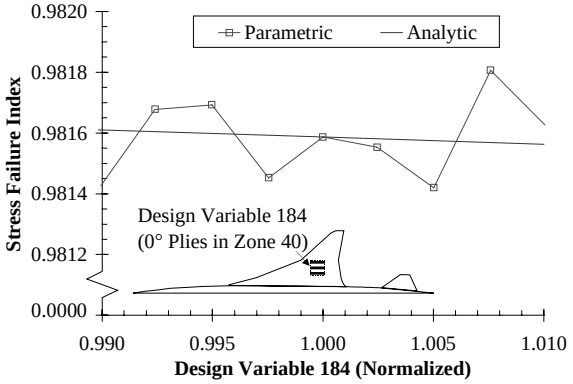

Fig. 16. SFI variation with design variable 184 for element 5140.

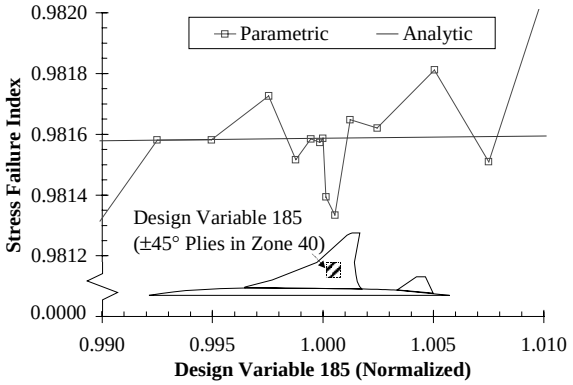

Fig. 17. SFI variation with design variable 185 for element 5140.

SFI responses for element 25035 (on the upper wing surface, see Fig. 11) are plotted in Figs. 18 to 23. The ranges of the SFI axes in Figs. 18 to 21 are identical for comparison purposes. The parametric SFI responses in Figs. 18 to 21 are nearly linear functions within the selected design variable range. Again, the slopes of the parametric SFI curves are different from the slopes of the analytic (uncoupled) SFI responses.

The ranges of the SFI axes in Figs. 22 and 23 are different than Figs. 18 to 21 because the sensitivities are smaller. Unlike the SFI sensitivities in Figs. 16 and 17, the sensitivities in Figs. 22 and 23 are larger than the numerical noise in the SFI variation. The larger sensitivities in Figs. 22 and 23 are because the thickness of element 25035 is sized by structural design variables 184 and 185. As in the earlier figures, the effect of the coupling term in the SFI sensitivities is larger for the shape variables than for the structural variables.

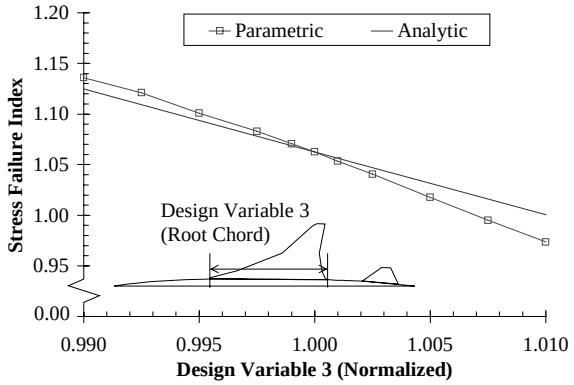

Fig. 18. SFI variation with design variable 3 for element 25035.

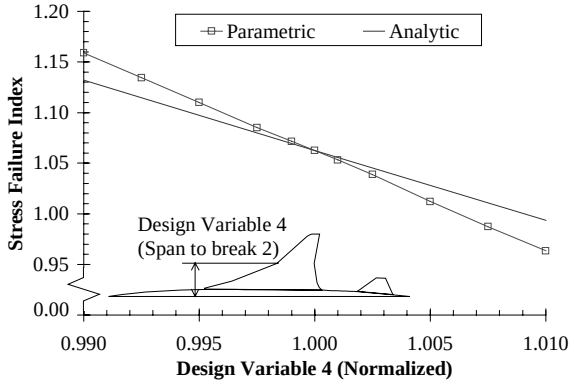

Fig. 19. SFI variation with design variable 4 for element 25035.

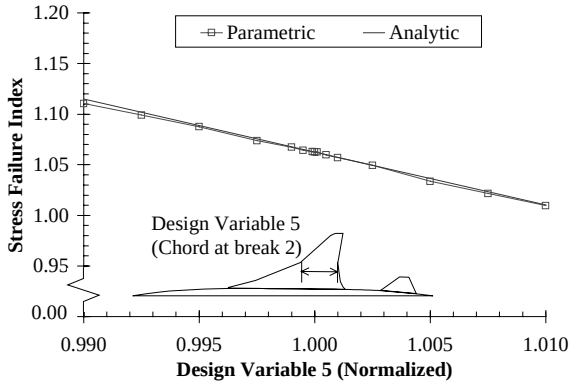

Fig. 20. SFI variation with design variable 5 for element 25035.

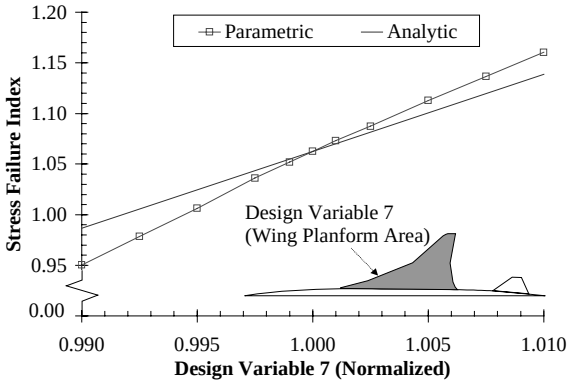

Fig. 21. SFI variation with design variable 7 for element 25035.

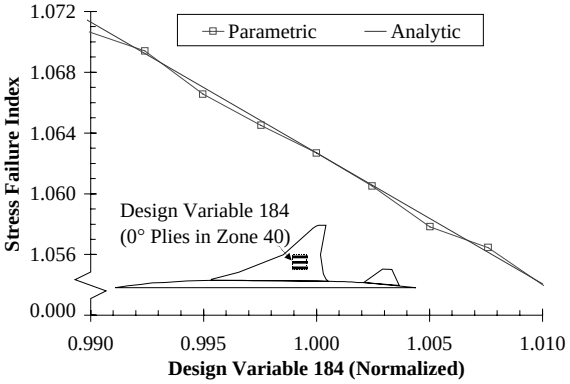

Fig. 22. SFI variation with design variable 184 for element 25035.

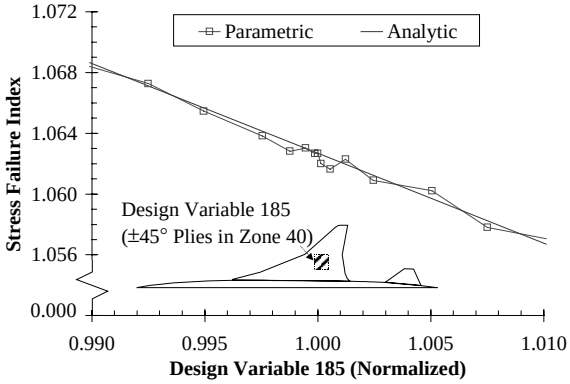

Fig. 23. SFI variation with design variable 185 for element 25035.

SFI responses for element 25082 (on the lower wing surface, see Fig. 11) are plotted in Figs. 24 to 29. The ranges of the SFI axes in Figs. 24 to 27 are identical for comparison purposes. The parametric SFI responses in Figs. 24 to 27 are nearly linear functions within the selected design variable range. Again, the slopes of the parametric SFI curves are slightly different from the slopes of the analytic (uncoupled)

SFI responses. The ranges of the SFI axes in Figs. 28 and 29 are magnified from Figs. 24 to 27 because the sensitivity of the SFI in the lower wing surface is much smaller with respect to changes in the upper wing surface (zone 40) ply thicknesses. As before, because the sensitivity with respect to variables 184 and 185 are very small, the effects of noise in the SFI response is more pronounced. As in the earlier figures, the effect of the coupling term (Equation 7) in the SFI sensitivities is larger for the shape variables than for the structural variables.

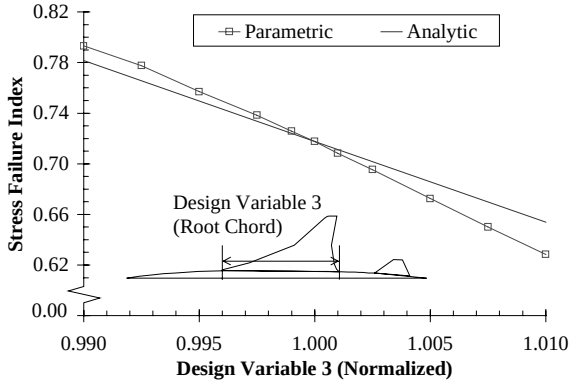

Fig. 24. SFI variation with design variable 3 for element 25082.

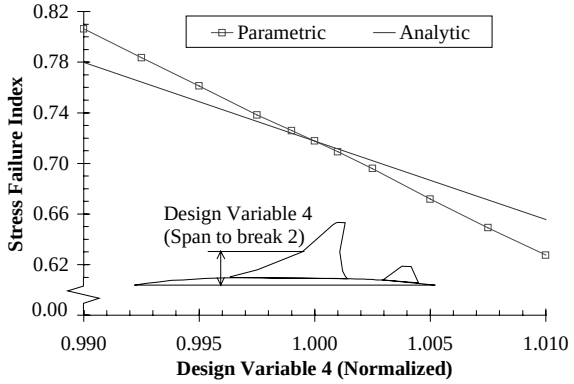

Fig. 25. SFI variation with design variable 4 for element 25082.

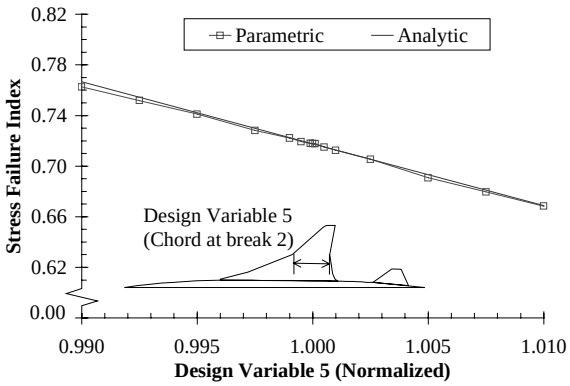

Fig. 26. SFI variation with design variable 5 for element 25082.

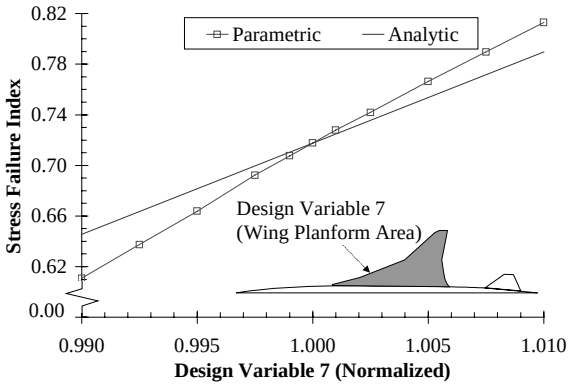

Fig. 27. SFI variation with design variable 7 for element 25082.

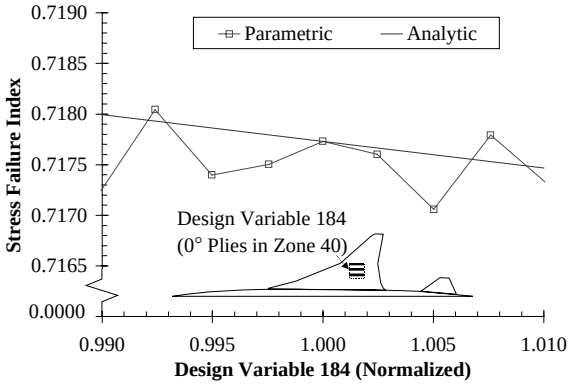

Fig. 28. SFI variation with design variable 184 for element 25082.

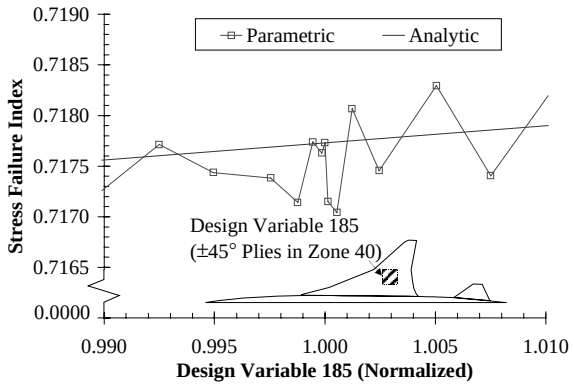

Fig. 29. SFI variation with design variable 185 for element 25082.

Performance of the analysis and sensitivity calculation methods is shown in Table 1. Computing the stress sensitivities with respect to all 271 design variables by finite differences requires 272 executions of the entire *Analysis* process, about 1768 hours. In comparison, the analytic (uncoupled) stress sensitivity calculation requires only 7.0 hours. Thus while not as accurate, the computational expense of the analytic (uncoupled) sensitivity calculation is much lower than finite difference sensitivities.

Table 1. CPU Time Required for Analyses

Process	CPU Execution Time (hrs.)		
	Analysis	Finite Difference Sensitivity	Uncoupled Stress Sensitivity
Aero.	6.10	1659.20	6.10
Disp.	0.37	99.73	0.37
Stress	0.03	9.07	0.03
$\partial Stress/\partial v$	0.00	0.00	0.50
Total	6.50	1768.00	7.00

Concluding Remarks

In this paper, a system for coupled aerodynamic and structural analysis of a HSCT using the ModelCenter® framework is presented. Formulations for weight and stress sensitivity derivatives are presented. The stress sensitivities are shown to constitute both uncoupled structural and coupled aero-structural derivative terms. Analytically computed GTOW sensitivities are shown to match slopes of parametric GTOW curves well. Parametric and analytic (uncoupled) stress responses are compared and demonstrate that the aero-structural coupling has a significant effect on the stress responses. The coupling effect is larger for the shape design variables than for the structural design variables. Further research is recommended in analytic calculation of the coupled terms in the stress sensitivities and in parallel execution of the HSCT4.1 system.

References

[1]Walsh, J. L., Townsend, J. C., Salas, A. O., Samareh, J. A., Mukhopadhyay, V., and Barthelemy, J.-F., "Multidisciplinary High-Fidelity Analysis and Optimization of Aerospace Vehicles, Part 1: Formulation," AIAA Paper 2000-0418, January 2000.

[2]Walsh, J. L., Weston, R. P., Samareh, J. A., Mason, B. H., Green, L. L., and Biedron, R. T., "Multidisciplinary High-Fidelity Analysis and Optimization of Aerospace Vehicles, Part 2: Preliminary Results," AIAA Paper 2000-0419, January 2000.

[3]Barthelemy, J.-F.M., Wrenn, G. A., Dovi, A. R., Coen, P. G., and Hall, L. E., "Supersonic Transport Wing Minimum Weight Design Integrating Aerodynamics and Structures," *Journal of Aircraft*, Vol. 31, No. 2, 1994, pp. 330–338.

[4]Giunta, A. A., and Sobieszczanski-Sobieski, J., "Progress Toward Using Sensitivity Derivatives in a High-Fidelity Aeroelastic Analysis of a Supersonic Transport," *Proceedings of the 7th AIAA/USAF/NASA/ ISSMO Symposium on Multidisciplinary Analysis and Optimization*, Part 1, St. Louis, MO, 1998, pp.441–453.

[5]Giunta, A. A. "Sensitivity Analysis for Coupled Aero-Structural Systems," NASA TM-1999-209367, August 1999.

[6]Sobieszczanski-Sobieski, J., "Sensitivity of Complex, Internally Coupled Systems," *AIAA J.*, 28(1), 1990, pp.153–160.

[7]Sistla, R., Dovi, A. R., Su, P., and Shanmugasundaram, R., "Aircraft Design Problem Implementation Under the Common Object Request Broker Architecture," *40th AIAA/ASME/ASCE/AHS/ASC Structures, Structural Dynamics, and Materials Conference and Exhibi*t, St. Louis, MO, 1999, pp. 1296–1305B.

[8]"Process Integration Using ModelCenter®," Technical White Paper, Phoenix Integration, Inc., Blacksburg, VA, 2000.

[9]Woodward, F. A., "USSAERO Computer Program Development, Versions B and C," NASA CR-3228, April 1980.

[10]Vanderplaats, G. N., *GENESIS® User's Manual, Version 5.0*, Colorado Springs, CO, 1998.

Appendix A - Unloaded Shape Computation

Both the geometry of the aerodynamic model used in the *Rigid Trim* process and the FEM used in the *Displacements* process are based on the 1-g cruise shape (s_C, see Fig. A-1), which is described by the shape design variables.

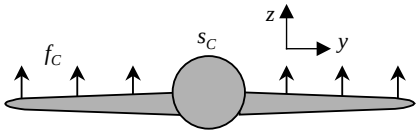

Fig. A-1. Cruise Shape.

In order to obtain accurate stress responses from a structural analysis, the displacements must be computed relative to the unloaded shape (s_0, see Fig. A-2). The unloaded shape is the aircraft shape that deforms to the cruise shape when cruise loads (f_C) are applied.

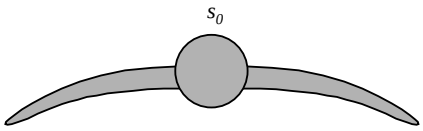

Fig. A-2. Unloaded Shape.

The cruise loads are computed from Equation A.1:

$$f_C = a_C - w_C \qquad \text{(A.1)}$$

where a_C represents the aerodynamic cruise loads, and w_C represents the inertial loads. The inertial loads (nodal cruise weight) are subtracted from a_C because the weight acts in the negative *z* direction.

The shape change (displacements) from the unloaded shape to the cruise shape is given by the following equation:

$$s_C - s_0 = u_0 = [K_0]^{-1} f_C \qquad \text{(A.2)}$$

Unfortunately, the stiffness matrix of the unloaded shape (K_0) is unknown. Assuming that the FEM is geometrically linear, the differences between the stiffness matrices of the unloaded shape (K_0) and the cruise shape (K_C) are negligible. Using this assumption, the cruise loads (f_C) can be applied to the cruise shape stiffness matrix (K_C) to produce a set of cruise displacements (u_C).

$$u_c = [K_C]^{-1} f_C = [K_0]^{-1} f_C = u_0 \qquad \text{(A.3)}$$

Thus, the unloaded shape is given by the cruise shape (s_C) minus the cruise displacement vector (u_C).

$$s_0 = s_C - u_C = s_C - u_0 \qquad \text{(A.4)}$$

Appendix B - Loads Convergence

In this appendix, load conditions 2 through 7 are referred to as maneuver conditions, and the corresponding loads are converted to forces acting at FEM nodes. At maneuver conditions, the aircraft has shape s_M and is subjected to maneuver loads f_M (illustrated in Fig. B-1).

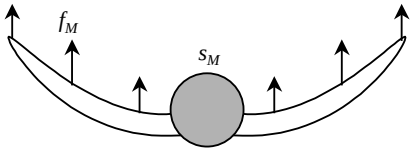

Fig. B-1. Maneuver Shape.

The maneuver loads are computed from Equation B.1:

$$f_M = a_M - LF\ w_M \qquad \text{(B.1)}$$

where a_M represents the aerodynamic maneuver loads; *LF* represents the maneuver load factor, and w_M represents the nodal weight at maneuver conditions (GTOW). The *Weights* process is used to compute the nodal GTOW. The inertial loads (*LF* multiplied by nodal GTOW) are subtracted from a_M because the weight acts along the negative *z* direction.

The maneuver shape (s_M) and aerodynamic maneuver loads (a_M) are unknowns that are determined using the *Loads Convergence* process. The maneuver shape is the net aircraft shape used for the aerodynamic analysis and consistent with the deformed structural shape produced by the aerodynamic loads.

The maneuver displacements are produced by deforming the unloaded shape (s_0) to the maneuver shape (s_M) as illustrated in Fig. B-2.

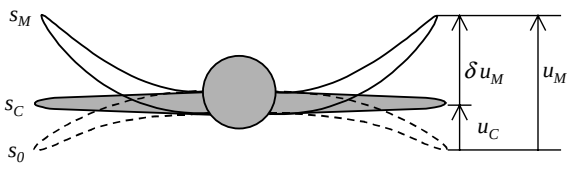

Fig. B-2. Delta Displacements.

The maneuver displacements (u_M) are computed using equation B.2:

$$u_M = s_M - s_0 = [K_0]^{-1} f_M \qquad \text{(B.2)}$$

The unloaded stiffness matrix (K_0) is unknown, but by applying the geometric linearity assumption from Appendix A, the cruise stiffness matrix (K_C) can be used in place of K_0 to calculate the maneuver displacements (u_M).

$$u_M = s_M - s_0 = [K_C]^{-1} f_M \qquad \text{(B.3)}$$

In the aerodynamics analysis, the maneuver shape (s_M) must be used to compute the aerodynamic maneuver forces (a_M). The maneuver shape is obtained by perturbing the existing aerodynamic model, which is based on the cruise shape (s_C). The displacements (referred to as "delta displacements," δu_M) used to perturb the aerodynamic model are computed from equation A.4 (in Appendix A) and equation B.3.

$$\begin{aligned} \delta u_M &= s_M - s_C = (s_M - s_0) - (s_C - s_0) \\ &= u_M - u_C \end{aligned} \qquad \text{(B.4)}$$